HAL
open science

Scavenging of ultrafine particles by rainfall at a boreal site: observations and model estimations

C. Andronache, T. Grönholm, L. Laakso, V. Phillips, A. Venäläinen

To cite this version:

C. Andronache, T. Grönholm, L. Laakso, V. Phillips, A. Venäläinen. Scavenging of ultrafine particles by rainfall at a boreal site: observations and model estimations. Atmospheric Chemistry and Physics Discussions, 2006, 6 (3), pp.3801-3844. hal-00303906

HAL Id: hal-00303906

https://hal.science/hal-00303906v1

Submitted on 18 Jun 2008

HAL is a multi-disciplinary open access archive for the deposit and dissemination of scientific research documents, whether they are published or not. The documents may come from teaching and research institutions in France or abroad, or from public or private research centers.

L'archive ouverte pluridisciplinaire **HAL**, est destinée au dépôt et à la diffusion de documents scientifiques de niveau recherche, publiés ou non, émanant des établissements d'enseignement et de recherche français ou étrangers, des laboratoires publics ou privés.

Atmos. Chem. Phys. Discuss., 6, 3801–3844, 2006
www.atmos-chem-phys-discuss.net/6/3801/2006/
© Author(s) 2006. This work is licensed
under a Creative Commons License.

Atmospheric Chemistry and Physics Discussions

Scavenging of ultrafine particles by rainfall at a boreal site: observations and model estimations

C. Andronache[1], T. Grönholm[2], L. Laakso[2], V. Phillips[3], and A. Venäläinen[4]

[1]Boston College, Chestnut Hill, Massachusetts, 02467 USA
[2]Department of Physical Sciences, University of Helsinki, P.O. Box 64, 00 014 Helsinki, Finland
[3]Princeton University, Atmospheric and Oceanic Sciences Program, Princeton, New Jersey 08540, USA
[4]Climate and Global Change Finnish Meteorological Institute Erik Palménin aukio 1, 00 560 Helsinki P.O. Box 503, 00 101 Helsinki, Finland

Received: 16 December 2005 – Accepted: 20 January 2006 – Published: 12 May 2006

Correspondence to: C. Andronache (andronac@bc.edu)

Abstract

Values of the scavenging coefficient were determined from observations of ultrafine particles (with diameters in the range 10–510 nm) during rain events at a boreal forest site in Southern Finland between 1996 and 2001. The estimated range of values of the scavenging coefficient was $[7\times10^{-6}–4\times10^{-5}]\,s^{-1}$, which is generally higher than model calculations based only on below-cloud processes (Brownian diffusion, interception, and typical charge effects). A new model that includes below-cloud scavenging processes, mixing of ultrafine particles from the boundary layer (BL) into cloud, followed by cloud condensation nuclei activation and in-cloud removal by rainfall, is presented. The effective scavenging coefficients estimated from this new model have values comparable with those obtained from observations. Results show that ultrafine particle removal by rain depends on aerosol size, rainfall intensity, mixing processes between BL and cloud elements, in-cloud scavenged fraction, in-cloud collection efficiency, and in-cloud coagulation with cloud droplets. Implications for the treatment of scavenging of BL ultrafine particles in numerical models are discussed.

1 Introduction

Aerosol particles are generated in the atmospheric environment by homogeneous nucleation of gaseous species, and by ion-induced nucleation (Covert et al., 1992; Widensohler et al., 1996; Raes et al., 1997; Weber et al., 1998; Kulmala et al., 1998, 2000a, 2004; Allen et al., 1999; O'Dowd et al., 1999; Birmili and Widensohler, 2000; Yu and Turco, 2001). Also, nucleation mode particles are emitted from gasoline engines (Harris and Maricq, 2001). Aitken mode particles are emitted directly from traffic exhaust, or may result from condensational growth of nucleation mode particles (Kerminen and Wexler, 1996; Alam et al., 2003, Laakso et al., 2003b). Accumulation mode particles originate from industrial combustion and re-suspension from road beds. Some aerosols originate from sea spray and cloud processing of particles and vapours). Par-

ticles larger than 100 nm are mainly mechanically generated: dust, re-suspension, industrial processes and sea-salt.

Ultrafine particles (UFP) are generally defined as aerosols with diameter d_p<100 nm. In this work, we will use UFP to describe the full range of available aerosol size [10–510] nm from the analyzed measurements (Laakso et al., 2003a). Homogeneous nucleation and direct injection of ultrafine particles (UFP) into the atmospheric environment both act to increase particle concentrations during pollution events. This affects visibility, cloud-condensation nuclei (CCN), and human health. After their formation, the fate of UFP is controlled by a combination of processes: advection, turbulent mixing, coagulation, condensation-evaporation, chemical reactions, aerosol-cloud interactions, and deposition (Seinfeld and Pandis, 1998; Jacobson, 2002). The sizes of UFP are augmented by the processes of condensation and coagulation, while their number concentration is reduced by coagulation with pre-existing aerosol particles and by various deposition processes. Kulmala et al. (2000a) showed that UFP with diameters, d_p~1–10 nm, are efficiently scavenged by Brownian coagulation with larger ambient aerosols. The growth of UFP to sizes, d_p~10 nm, is critical for the survival of such particles and for their potential influence on CCN concentrations. To become activated as cloud droplets, UFP need sufficient time to grow by condensation and coagulation. Rain is an effective mechanism for aerosol removal from the atmosphere and it can limit the number of small aerosol particles growing to the sizes required for activation of cloud droplets. Atmospheric particles removal is also a process of interest for numerical studies, in the effort to improve aerosol and chemical models at various scales (for example, see Rasch et al., 2000; Tost et al., 2006).

The wet removal of aerosol particles (AP) from atmosphere is caused by two processes: (a) if an AP is in the BL below-cloud, it can be collected by a falling raindrop ("below-cloud scavenging", BCS); (b) if an AP is in-cloud or at cloud base, where supersaturated conditions exist, it can become a cloud droplet by the nucleation scavenging process (Komppula et al., 2005). Such a particle grows to the size of a cloud droplet and can be efficiently collected by raindrops falling inside cloud ("in-cloud scavenging",

ICS). In-cloud interstitial aerosol can be also be scavenged by coagulation with cloud droplets and by collection onto falling raindrops.

The below-cloud scavenging rate depends on the collection efficiency between a falling raindrop and aerosol particles. Throughout this paper we assume that the collection efficiency is equal to the collision efficiency. This assumption is correct if every collision between a UFP and a raindrop is followed by coalescence. It has been shown (Pruppacher and Klett, 1998) that a collision is followed by coalescence when $d_p/D_p \ll 1$, where D_p is the raindrop diameter. This is because, in that case, the kinetic energy of tiny aerosol particles is relatively small in comparison with that of large particles (falling raindrops), causing the probability of bounce-off in collisions between small UFP and raindrops to be low. In that sense, the coalescence efficiency of UFP colliding with raindrops must be close to unity. The condition for coalescence during a collision is satisfied by typical UFP present in the BL below-cloud, where aerosol particles uptake water and become wet. These UFP behave as small spherical particles colliding with a falling raindrop.

Brownian diffusion is an efficient mechanism for collection of very small particles (with diameters $d_p \leq 10$ nm) by falling raindrops (Greenfield, 1957). Similarly, large particles (with diameters $d_p \geq 2000$ nm) have a relatively high collection efficiency because of their inertia, while particles with diameters in the range 10 nm $\leq d_p \leq 2000$ nm ("Greenfield gap"), tend to have small collection efficiencies. Slinn and Hales (1971) showed that thermophoresis could enhance the below-cloud scavenging of aerosols with diameters in the range [10–1000] nm. Work by Grover et al. (1977), Wang et al. (1978), McGann and Jennings (1991), Byrne and Jennings (1993), Tinsley et al. (2000), showed that presence of electric charge on aerosol particles and raindrops increases the below-cloud scavenging of aerosols with sizes in the "Greenfield gap".

A series of studies estimated the effects of below-cloud scavenging on aerosol size distribution under various environmental conditions (Dana and Hales, 1976; Wang and Pruppacher, 1977; Slinn, 1983; Ten Brink et al., 1987; Jylhä, 1991; Sparmacher et al., 1993; Andronache, 2003). Several reports estimated aerosol scavenging coefficients

from direct measurements of the AP size distribution change at ground stations during rain events (Davenport and Peters, 1978; Schumann 1991; Laakso et al., 2003a; Chate and Pranesha, 2004; Maria and Russell, 2005). Scavenging rates determined from such measurements show a large spread, and tend to be significantly higher than estimations based only on below-cloud collection removal. Such results suggest that other processes are important in determining the overall observed scavenging of UFP from the BL. To address this problem, the present study has the following goals: (1) to present the data and characteristics of aerosol observations during rain events at a boreal station in Finland, with implications for UFP scavenging; (2) to describe a modeling framework that accounts for below-cloud scavenging, UFP mixing into the cloud domain, nucleation scavenging and in-cloud scavenging, so as to estimate the UFP effective scavenging coefficient. The study discusses the dependence of UFP scavenging on environmental parameters, with implications for aerosol numerical models and future field studies.

2 Observations

To determine the rate of scavenging of UFP during rain events, we used data from six years (1996–2001) measurements at SMEAR II Station (Station for Measuring Forest Ecosystem-Atmosphere Relations), Hyytiälä, Southern Finland (61°51′ N, 24°17′ E; 181 m a.s.l.) (Vesala et al., 1998) (Fig. 1). The station is located in a homogeneous Scots pine forest and is characterized by typical background conditions, with no local sources of pollution (Kulmala et al., 2000b). The particle size distributions between 3 and 510 nm have been measured by two differential mobility particle sizers (DMPS). The combination of the two instruments provided, for each 10 min period, the particle classification in 29 logarithmically distributed size channels between the diameters of 3 and 510 nm (Aalto et al., 2001). Rain was observed by the tipping bucket method with an ARG100 rain gauge and the final data was stored at a time resolution of 15 min.

Only data from the period between 1 May and 31 October of each year from 1996

to 2001 were used. This avoided contamination of the data by scavenging onto snow, and also eliminated errors in rain measurements caused by frozen measurement devices. The analysis was also limited to particles with $d_p \geq 10$ nm because the concentration of smaller particles is generally too low during rain events and instrumental errors can be significant. Another reason for this lower limit on particle diameter is that there is the possibility of condensational growth of nanometer-sized particles. For the same reason, cases with visible growth of particles were rejected. Analysis of the data was started by selecting rain events that lasted at least 0.5 h with a rain intensity $R \geq 0.4\,\mathrm{mm\,h^{-1}}$. Smaller values of R were rejected because of possible inaccuracy of the rain gauge at low rain intensities. The limitation on rain duration arises from the needs both for accuracy in individual rain measurements and for sufficient spatial coverage of sampling network of rain observations, such that robust statistical results may be achieved.

Figure 2 illustrates time series of $\mathrm{d}n/\mathrm{dlog}(d_p)$ (for two particle diameters: 32 nm and 340 nm) and accumulated precipitation at intervals of 15 min, for the year 2000. Dry periods are excluded from this plot and the continuous line is used only to increase the clarity of the plot. UFP number concentrations at various diameters do not show a simple correlation, and the variability is high. A scatterplot of $\mathrm{d}n/\mathrm{dlog}(d_p)$ (for two particle diameters: 32 nm and 340 nm) versus rainfall rate is shown in Fig. 3 for years 1998–2001. First, we note a substantial decrease of number concentration at any of the two selected diameters with the increase in rain intensity (The same result is seen at all UFP diameters). Second, the plot shows the predominance of cases with small rainfall rates $\sim 1\,\mathrm{mm\,h^{-1}}$. The number of samples with $R \geq 10\,\mathrm{mm\,h^{-1}}$ is almost negligible. During each rain event that has been analyzed, the measured size distribution of UFP changes in time. If wet removal were the only process acting on the aerosol population, we would see a decrease in aerosol concentration with time, over the duration of the rain event. Often, other processes alter the size distribution, and measurements show cases in which aerosol concentration can grow during precipitation. Such effects may be attributed to processes such as advection, mixing, and growth. An example of

a change in the UFP size distribution with time is shown in Fig. 4 for a case observed on 9 October 1999. The rain event lasted 3 h, with $R \sim 1\,\mathrm{mm\,h^{-1}}$, an air temperature between 6–9°C, and a horizontal wind speed $\sim 1\,\mathrm{ms^{-1}}$. We see a continuous decrease of the size distribution over most of the range of particle diameter, except for $d_p \leq 30$ nm where there is a modest increase in number concentration. This example illustrates the complexity of wet removal during a relatively extended rain event.

To avoid rapid changes in particle concentration caused by advection in frontal zones, rain events with strongly changing meteorological parameters such as temperature, pressure, wind speed and wind direction were rejected. Particle concentrations could change due to horizontal advection as well as due to vertical mixing and convection. Possible effects of vertical mixing could not be analyzed in the observed data but will be discussed in the model section. Significant changes in relative humidity also provided a criterion for rejecting rain events as it may cause important hygroscopic growth of particles. The role of hygroscopic growth is analyzed in the model section using a growth factor (GF) determined from observations and described in detail by Laakso et al. (2004). Turbulent fluctuations in concentration could not be avoided. Since each concentration measurement lasts only 20 s, turbulent fluctuations are not averaged out and act to increase the standard deviation of the scavenging coefficient.

As there are no local sources and nucleation has been observed only during sunny conditions (Mäkelä et al., 2000), nucleation is neglected during rain events. Significant nucleation was never observed during the selected rain events. Condensational growth of particles is assumed to be much smaller than the scavenging rates during each rain episode. The justification for this assumption is that: (1) data used in calculations do not include days when growth was clearly observed. (2) observed episodes of growth in Hyytiälä have been always related to photochemical reactions that are seen not to occur during periods of rain (Hyvönen at al., 2005). Coagulation of UFP is negligible in the BL, due to fast removal of larger particles by raindrop impaction and by nucleation scavenging (aerosol scavenging due to cloud droplet activation). By using the criteria of data selection described above, the remaining key factors that affect measured particle

concentrations are assumed to be turbulent mixing, instrumentation errors and various scavenging processes. Instrumental errors may lead to systematic or random errors, while turbulent fluctuations only contribute to random errors.

Analysis of meteorological data at Hyytiälä at 8.4 m above ground is illustrated in Fig. 5. Air temperature (Fig. 5a) varies between 0 and 25°C. The accumulated precipitation recorded during 15 min is mostly less than 1 mm, while the highest values reach ~5 mm during the warmest months of the summer when convective precipitation is more frequent. However, such convective precipitation events are not too intense overall, since they generally produced $R \leq 10\,\mathrm{mm\,h^{-1}}$. Rain duration (Fig. 5b) shows that the most frequent duration is less than 30 min, and there are very few cases with continuous rain events lasting more than 2–3 h. Figure 5c shows the distribution of horizontal wind intensity at 8.4 m, with values being predominantly in the range of 0.5–2.5 $\mathrm{ms^{-1}}$. Figure 5d shows the distribution of *RH* with values being mostly in the range of 90–100%. There are a few cases of *RH* in the range of 60–90% that are typically associated with the warmest periods and more intense precipitation events. Synoptic meteorological observations from Jokioinen (60°49′ N, 23°30′ E; 104 m a.s.l.) provide details on cloud and precipitation types during rainy intervals recorded both at Jokioinen and Hyytiälä. The statistics of precipitation at the two stations is similar, and therefore the precipitation events at Hyytiälä have similar properties as those observed at Jokioinen. Data from Jokioinen show that precipitating clouds extended over all altitudes, and precipitation was classified into two types: frontal or shower precipitation. This is consistent with the overall picture of widespread stratiform precipitation being predominant, in conjunction with less frequent convective events.

Based on these criteria of selection, the scavenging coefficient from observations, L_o was estimated from measurements of UFP number concentration using:

$$\frac{dn(d_p)}{dt} = -L_o n(d_p) \tag{1}$$

where $n(d_p)$ is the UFP number concentration, and d_p is the particle diameter. With $n(d_p)$ being measured at two times, t_1 and t_2, during rain events, the expression for

L_o becomes $L_o = -\frac{1}{(t_2-t_1)} \ln[\frac{n(t_2)}{n(t_1)}]$. The parameterization of L_o is described in detail by Laakso et al. (2003a), being summarized in the Appendix and illustrated in Fig. 6 for four rainfall intensities. Thus, L_o decreases with d_p in the range ~10–100 nm, has a minimum for d_p between 100–200 nm, and increases slightly for d_p larger than 200 nm. For any given aerosol diameter, L_o increases with rain intensity as $\sqrt{R}$. Shown are curves for R in the range 0.5–10 mm h^{-1}, which was typical for the samples utilised here. Significant variability was observed from case to case, and results shown in Fig. 6 must be seen as representative for average conditions of widespread precipitation and rain duration consistent with the resolution of R applied for the samples. These observed scavenging coefficients are compared with model results in the next section.

3 Model and results

Modeling of the rate of UFP scavenging observed in the BL near the ground during rain events must consider these processes: (a) raindrops falling below-cloud collect UFP with an efficiency that depends on the sizes of aerosols and raindrops; (b) over the duration of a rain event, BL UFP are mixed throughout BL and within clouds. Some particles become cloud droplets or coagulate with cloud droplets and are removed while inside clouds. In-cloud entrainment is a complex dynamic process that occurs at the cloud base, lateral boundaries, and the top of the cloud. The focus of the present study is on entrainment at cloud base and lateral boundaries that results in mixing UFP from the BL into cloud elements. Although during precipitation such a process is highly inhomogeneous spatially and the entrainment rate varies with time, it will be characterised here by average values of the following parameters: the entrainment velocity (w_e) at cloud base, the cloud base height (H), and the rain duration. Insight into the physics of entrainment is available from direct field measurements (Martin et al., 1994; Svenningsson et al., 1997; Snider and Brenguier, 2000), lidar data, high-resolution dynamic models, including large eddy simulations, and mesoscale models

applied for simulation of precipitation (Rutledge and Hobbs, 1983; Houze, 1993; Zhang et al., 2004). Such studies show significant variability of the parameters describing entrainment, and the important roles of turbulence and convection.

By adopting an average entrainment velocity and a cloud base height based on field data, we can estimate the fraction, f_1, of BL UFP reaching cloud base or being mixed into cloud. Once UFP reach cloud, where supersaturated conditions prevail, some particles become activated as cloud droplets by the nucleation scavenging process (Komppula et al., 2005). The scavenged fraction, f_2, depends on aerosol size, supersaturation and chemical composition, as will be discussed below. UFP, which are not affected by nucleation scavenging and are mixed into the cloud, are subject to coagulation with cloud droplets, which in turn have a high probability of being removed by raindrop collection.

With these considerations, the rate of change in the BL UFP due to precipitation is written as:

$$\frac{dn(d_p)}{dt} = -L_{BC}n(d_p) + \left(\frac{dn(d_p)}{dt}\right)_{\text{mix}} \tag{2}$$

where $n(d_p)$ is the BL UFP concentration, and L_{BC} is the below-cloud scavenging coefficient. The first term on the right-hand side of the above equation represents the loss of BL UFP by falling raindrops below cloud. The second term on the right-hand side represents the loss of BL UFP by mixing into cloud by entrainment, followed by nucleation scavenging and in-cloud scavenging.

The second term of the right-hand side of Eq. (2) is expressed as:

$$\left(\frac{dn(d_p)}{dt}\right)_{\text{mix}} = -f_2 L_{IC}^{\text{coll}} f_1 n(d_p) - L_{IC}^{\text{coag}} f_1 n(d_p) \tag{3}$$

where f_1 is the fraction of UFP from the BL that, by mixing and entrainment, reach cloud elements with supersaturated conditions. Also, f_2 is the fraction of such UFP that becomes activated as cloud droplets. L_{IC}^{coll} is the in-cloud scavenging coefficient due

to collection by raindrops inside cloud, and L_{IC}^{coag} is the in-cloud scavenging coefficient due to UFP coagulation with cloud droplets.

Thus, Eq. (2) can be written as:

$$\frac{dn(d_p)}{dt} = -L_{\text{eff}} n(d_p) \tag{4}$$

where $L_{\text{eff}}=L_{BC}+f_1 f_2 L_{IC}^{\text{coll}}+f_1 L_{IC}^{\text{coag}}$ is the effective (or apparent) scavenging coefficient of the BL UFP to be compared with L_o. Expressions for scavenging coefficients are given in Appendix A, and the list of notations is given in Appendix B.

3.1 Mixing of ultrafine particles into cloud

Entrainment of air and tracers into cloud depends on the intensity of vertical motions in the cloudy area, and has significant fluctuations over time and space. Since our goal is to explain the average behavior of the observed rate of scavenging, mixing of UFP into cloud will be characterised by typical entrainment parameters such as vertical velocity at cloud base w_b, cloud base height H, and rain duration t. Stratiform and convective precipitation are classified as follows. Stratiform precipitation falls from nimbostratus clouds, while convective precipitation falls from cumulus and cumulonimbus clouds (Houze, 1993). Stratiform precipitation is a process in which vertical air motions are small compared with the fall velocity of ice crystals and snow ($\sim$1–3 ms^{-1}). The vertical velocity at cloud base for stratiform clouds is $w_b\sim$0.2–0.5 ms^{-1} based on detailed studies of frontal stratiform precipitation (Rutledge and Hobbs, 1983). Convective precipitation has a vertical velocity in the range 1–10 ms^{-1}, which exceeds the typical fall speeds of snow and ice crystals.

For precipitation in Southern Finland that occurred during the sampling period, rain events are characterized by short durations ranging from less that 0.5 h to a few hours. Rainfall intensities were $R\sim$0.4–10 mm h^{-1}, with values mostly being less than 1 mm h^{-1} (Fig. 3). Inspection of the precipitation data from Jokioinen shows that frontal systems moving from Atlantic region over the southern Finland during summer cover a

large area dominated by low R. Embedded in the frontal systems are convective precipitation systems occupying a smaller area, where R can be significantly higher. Often such frontal systems present a band structure that results in rain events interrupted by intervals of no rain or insignificant precipitation. Thus, for the time average of R in this experiment (15 min), the dominant precipitation is stratiform in nature, and convective cases are rare or are excluded from the analysis (Laakso et al., 2003a).

To estimate the fraction of UFP from the BL that reaches cloud base, f_1, it is assumed that UFP are well mixed within the BL. It is also assumed that as such particles reach the cloud domain or free troposphere, they are removed by in-cloud processes without being mixed back into the BL. We note that while w_b at cloud base (averaged over sufficient temporal and spatial extent to represent a mesoscale or synoptic event) has a positive value ($\sim$0.2–0.5 ms^{-1}), the vertical velocity at the ground is zero. Assuming a linear increase of vertical velocity between the ground and cloud base (at height H), the average vertical velocity w in the BL is $w \sim \frac{w_b}{2}$, a value that is applied in these estimations. The mixing process in the BL is assumed to be independent of UFP size, and there is experimental evidence for the aerosol particle concentration being approximately constant throughout the BL (Pimenoff et al., 2005). Thus, the change in UFP number concentration due to mixing is $\frac{dn}{dt} = -\frac{w}{H} n$, with the solution being $n(t) = n(0)\exp(-t/\tau)$ where $\tau = \frac{H}{w}$. The fraction of UFP lost from the BL during time t is $f_1 = \frac{n(0)-n(t)}{n(0)}$, where $n(0)$ and $n(t)$ are the UFP number concentration at beginning of rain and after a time t. The fraction f_1 is plotted in Fig. 7 versus w, for three values of H for a rain duration of 0.5 h. Note that f_1 increases with w, and in real situations, variability is expected. f_1 values illustrated here do not apply for convective, intense precipitations, where f_1 can be higher and the mixing of UFP back from the free troposphere into the BL can be significant.

3.2 In-cloud nucleation scavenging

When aerosol particles reach the cloud base by mixing and are entrained into the cloud element, they encounter supersaturated conditions. A fraction, f_2, of such particles is then activated and form cloud droplets. Now, f_2 is often named the scavenged fraction or scavenged ratio (Svenningsson et al., 1997; Martinsson et al., 1999, Komppula et al., 2005). This is the process by which cloud droplets form on pre-existing aerosol particles. Under subsaturated conditions, aerosol particles have equilibrium sizes determined by the ambient relative humidity (*RH*) and the amount of soluble matter in the particle. At supersaturated conditions, particles can grow larger than the critical diameter and form cloud droplets. The supersaturation required for droplet activation depends mostly on the aerosol size and to a lesser extent on the chemical composition of the aerosol particle. The supersaturation is governed by the rate of cooling of the air mass and the rate of condensation of vapour on the growing droplets. As a result, cloud formation causes a group of activated cloud droplets and another group of interstitial aerosol particles that both co-exist. The interstitial aerosol particles contain liquid or dry particles of equilibrium size (with diameters much smaller than cloud droplets). The study of aerosol hygroscopic behavior, aerosol activation, aerosol scavenged fraction, and cloud microphysics characteristics were extensively investigated in a series of field experiments and with numerical models (Martin et al., 1994; Garrett and Hobbs, 1995; Twohy et al., 1995; Svenningsson et al., 1997; Martinsson et al., 1999; Swietlicki et al., 1999; Väkevä et al., 2002; Komppula et al., 2005).

For a given local supersaturation S, the nucleation scavenging of AP is determined by the size and chemical composition of aerosols. Experimental determination of the scavenged fraction reveals the complexity of the nucleation scavenging process, owing to variations in S locally and in the chemical nature of AP (Martinsson et al., 1999; Komppula et al., 2005). Thus, for the same supersaturated conditions, some particles with diameters as low as 50 nm become activated, while a small fraction of particles with $d_p \geq 200$ nm can remain unactivated. The scavenging fraction tends to increase

rapidly with d_p at diameters around 100 nm. Model simulations of soluble aerosol, with an updraft velocity that produces local supersaturations of ~0.1–0.2%, predict a sharp increase of f_2 with particle diameter (Svenningsson et al., 1997). To account for possible variability in aerosol chemical composition and variations in S, we adopt an f_2-function (Fig. 8) that summarizes experimental results by Martinsson et al. (1999) and Komppula et al. (2005). The thick black curve represents the f_2-function used for the standard run to be compared with L_o. The blue lines show the range of f_2 data reported by Martinsson et al. (1999) are based on observations from air masses with predominantly continental influences, occasionally impacted by pollution, as reflected in the observed large number concentration of cloud droplets. The red dotted lines with symbols represent the range of f_2 based on data reported by Komppula et al. (2005) for the station Pallas in Northern Finland, a pristine continental site, often impacted by clean maritime air masses. Data from the two studies overlap for conditions specific to continental air masses, while the red curve with rhombic symbols from Komppula et al. (2005) is more representative for clean maritime air masses. We choose f_2 to approximate typical continental air masses because at Hyytiälä, the impact of continental influences is more significant than at Pallas.

3.3 In-cloud collection and coagulation scavenging

The UFP that undergo nucleation scavenging grow to cloud droplet size and are removed by falling raindrops inside clouds. This leads to a scavenging coefficient L_{IC}^{coll} given in Appendix A. The physics of this process is the following: as UFP are drawn into the cloud, they are activated as CCN and grow to a cloud droplet size with a diameter ~10 μm. The collection efficiency E_{IC} for cloud droplets of 10 μm in diameter varies between 0.5 and 0.8 when the collectors are raindrops with diameter D_p~0.2–2 mm (Slinn, 1977). These considerations apply also for highly soluble aerosol, or aerosol attached to material that is highly soluble, such that particles can grow to a droplet size. For aerosol that is less soluble, the collection efficiency can be lower than 0.5. For snow, E_{IC}~0.1–0.3, based on estimations by Scott (1982).

Another aspect of the in-cloud collection by rainfall is the vertical variation of rainfall intensity R. Measurements usually only yield R values at the ground. Scott (1982) shows that for summer precipitations, R measured at the ground is representative of the BL, while above the cloud base, R decreases with height and becomes negligible at z~6–7 km. Thus, we estimated that average in-cloud rainfall intensity, R_{IC}, is about half of the ground value, R.

The second important mechanism of in-cloud removal of UFP is for the small UFP that are not affected by nucleation scavenging (mostly with $d_p \leq 100$ nm). These particles can coagulate with cloud droplets, raindrops or remain as interstitial aerosol. It can be shown that UFP coagulation with raindrops is insignificant because the number concentration of raindrops is much lower than that of cloud droplets. UFP coagulation with cloud droplets is important, and can lead to inclusion of UFP into droplets, followed by raindrop collection. This process leads to a scavenging coefficient, L_{IC}^{coag}, described in Appendix A.

3.4 Effective scavenging coefficient

With these considerations, a reference run to estimate the effective scavenging coefficient L_{eff} was produced based on the following numerical values of various parameters: R=1 mm h^{-1}, t_c=10°C, N_0=8×10^{6}m^{-4}, E_{IC}=0.5, f_1=0.1, N_c=500 cm^{-3}, d_c=10 μm. Table 1 summarizes several model parameters, their values used in the reference run and the range of values used in sensitivity calculations. Estimated values of L_{eff} from the model are shown in Fig. 9 for neutral and charged particles, at two values of the relative humidity, RH=60% and RH=99%. Model predictions of L_{eff} are comparable with L_o from observations. The black dashed lines represent approximations of L_o uncertainty from observations. The role of electric charge does not seem significant, and it is reasonable to assume that this mechanism is not important for predominantly stratiform precipitation based on reported data (Pruppacher and Klett, 1998). The Coulomb interaction for average charge is important for thunderstorms and highly electrified clouds, becoming more evident at high values of R (associated with convective precipitation).

The possible effect of image charges can be important as well but it is not included in this model. The presence of ions at SMEAR II (Laakso et al., 2004), and work by Tinsley et al. (2000), Tripathi and Harrison (2001), Harrison and Carslaw (2003) indicate that electrostatic charge image interaction is possible between AP and raindrops. There is not yet a direct experimental account of the role of electric charge in UFP scavenging, and in the rest of the paper we will show results only for neutral particles.

The effect of the growth factor (GF) of UFP is important for determining which particles become activated by nucleation scavenging. GF has less effect on very small particles that coagulate with cloud droplets because GF is at most ~2 while between UFP diameters and cloud droplets there is a size difference of orders of magnitude. Thus coagulation between UFP and cloud droplets is not affected greatly by GF. Similarly, for UFP with $d_p \geq 100$ nm, in-cloud scavenging is less sensitive to further growth in diameter and we see less impact of GF on the overall scavenging of particles larger than 100 nm. The highest effect of the growth factor is seen for d_p in the range 50–100 nm where GF can make a significant difference. Thus, while a dry UFP of d_p=50 nm has a small scavenged fraction, after the size change due to the GF, such particle becomes closer to 100 nm and can be scavenged more effectively.

The effect of air temperature on UFP scavenging is low for liquid precipitation. Caution is needed when using the model for cases when t_c near the ground is close to 0°C. In such cases, it is possible that at higher altitudes, precipitation inside cloud is solid and the collection efficiency as well as the hydrometeor size distribution in cloud might be different. Based on criteria for data selection, the possible number of cases with low t_c is small and the overall scavenging coefficient is determined by scavenging onto liquid raindrops. The choice of value for N_0 is based on the standard Marshall and Palmer raindrop size distribution parameters (described in Appendix A), but we note possible large variations of this parameter and sensitivity of results will be shown below.

Figure 10 shows the model sensitivity with respect to the fraction, f_1, of UFP from the BL that are mixed into cloud elements. The value of f_1 increases with average vertical

velocity over the precipitation area, and is linked to a higher percentage of convective elements and to increased rainfall rates, R. The fraction f_1 is varied between 0.1 and 0.3 in this calculation, and other parameters are maintained at the constant values used for the simulations presented in Fig. 9. A larger increase of f_1 will require a higher value of R because intense vertical transport is generally associated with convective precipitation. It is possible in principle to use a detailed mesoscale model and estimate f_1 over an area of interest, correlating it with the measured or estimated rainfall rate, R, at the ground. Since the mixing of UFP is practically independent of aerosol size, this parameter influences all aerosol-cloud interactions described above (nucleation scavenging, in-cloud coagulation and collection). Thus, L_{eff} values increase with f_1 for the the entire range of UFP diameters.

Figure 11 shows model L_{eff} sensitivity to in-cloud collection efficiency E_{IC}. This parameter is varied between 0.3 and 0.9. For liquid precipitation, small values of E_{IC} (~0.1–0.3) are associated with less soluble aerosol, fresh soot or combustion aerosol. Such cases are related to air masses originating from the continent, perhaps passing over significant sources of combustion particles. Small E_{IC} values are also associated with solid precipitation. The E_{IC} values for snow are much smaller (~0.1–0.3) based on Scott (1982) and consistent with the results of Slinn (1977). Based on the temperature distribution near the ground for the samples used, the number of cases with possible snow precipitation in-cloud is quite limited and the overall influence on L_o is low as well. Thus, the sensitivity of model calculations to E_{IC} was limited to the range of 0.3–0.9. Note the remarkable sensitivity of estimated values of L_{eff} with respect to the in-cloud collection efficiency, especially for particles with $d_p \geq 50$ nm.

Figure 12 shows model sensitivity of L_{eff} with respect to number concentration N_c of cloud droplets. In the reference run we use $N_c = 500\,\mathrm{cm}^{-3}$, which is quite typical for continental clouds. Possible influences from polluted air masses over Europe causes higher number concentrations of cloud droplets (and lower average diameters of cloud droplets). We varied N_c between 500 and $1500\,\mathrm{cm}^{-3}$, which is consistent with data from field experiments that characterized cloud microphysics (Martinsson et al., 1999).

For maritime stratiform clouds, N_c is considerably lower, in the range 100–200 cm^{-3} (Martin et al., 1994). Overall, the increase of N_c tends to increase UFP removal by coagulation, assuming the average diameter does not change considerably. In fact, the average diameter of cloud droplets changes with the number concentration of droplets: larger N_c leads to smaller cloud droplets, which have slightly lower rates of coagulation with UFP. The sensitivity with respect to changes in cloud droplet diameter (not shown) indicates a similar range of variation of L_{eff}.

Finally, Fig. 13 illustrates model sensitivity of L_{eff} with respect to N_0, the intercept parameter of the Marshall-Palmer size distribution of raindrops. The standard value for N_0 is considered representative and stable for long term averages of the widespread precipitation. Field data show that N_0 can vary significantly (Pruppacher and Klett, 1998), and we illustrate the impact on model results caused by variations of one order of magnitude. Generally, L_{BC} is quite sensitive to N_0, which is reflected in the overall estimate of L_{eff}, especially for UFP with $d_p \leq 100$ nm.

The model results shown above, indicate reasonable agreement between calculated L_{eff} and observed values L_o for the UFP scavenging coefficient. For practical purposes, to account for the observed UFP removal near ground, the use of L_o is recommended within the UFP diameter range ($10 \leq d_p \leq 500$ nm) and rainfall intensity range ($0.4 \leq R \leq 10$ mm h^{-1}). Table 2 shows L_o reported from several field experiments in various places. Among these results, the one obtained from Hyytiälä is based on the largest data set available. Discrepancies between values in different experiments are due to rainfall intensity range and precipitation type. For example, data from Chate and Pranesha (2004) are determined from thunderstorm rain events, and the effect of electric charge can be important. For modeling purposes, the use of a simplified L_o fit from observations is also suitable, especially for pollution studies, while it is recommended to have L_o determined from data measured in the region of interest.

4 Conclusions

Scavenging coefficients were determined from six years of ultrafine particle (UFP) observations during rain events at a boreal forest site in Southern Finland. The range of the median scavenging coefficients was $[7\times10^{-6}-4\times10^{-5}]\,s^{-1}$, comparable with results from similar experiments, for the same rainfall rates. A model of UFP scavenging during rain events is described, based on these processes: (1) UFP below-cloud scavenging by falling raindrops; (2) UFP mixing in-cloud and nucleation scavenging; and (3) UFP in-cloud collection and in-cloud coagulation with cloud droplets. Model results show overall reasonable agreement with observed values (within the range of experimental uncertainties). Nevertheless, significant sensitivity to parameters related to mixing and cloud microphysics is expected. These results are applicable to predominant stratiform precipitation that is not too intense ($R\sim0.4-10\,mm\,h^{-1}$).

Our results suggest that the net loss of UFP near the ground during a rain event is the result of below-cloud scavenging due to aerosol collection by raindrops, mixing, cloud droplet activation and in-cloud scavenging. The importance of each process is determined by the mixing between BL and cloud elements. If the mixing is reduced, then the below-cloud scavenging caused by raindrop collection, is important. However, for typical mixing during rain event, the in-cloud processes are dominant, and can impact directly the overall UFP scavenging from the BL.

Model results show that ultrafine particle removal from the BL by rain depends on aerosol size, rainfall intensity, mixing processes between BL and cloud elements, the in-cloud scavenged fraction, the in-cloud collection efficiency, and in-cloud coagulation with cloud droplets. The chemical composition and aerosol history of chemical processing can impact the growth factor, possibly affecting the scavenged fraction of those particles that reach supersaturation conditions. Other effects related to electric charge may affect also the overall scavenging by increasing the efficiency of collection. The role of electric charge needs to be further investigated by direct measurements and by refining of current models of scavenging.

Future work to improve characterization of the scavenging coefficients, and our ability to estimate the loss of BL aerosol by precipitation, needs to include measurements of cloud hydrometeor properties such as vertical profiles of rainfall, raindrop size distributions, cloud vertical extent, cloud base height, and electric charge. Mesoscale models can be used to infer rates of mixing between BL and cloud region. The work needs also to be extended for snowfall precipitation, which is relevant in winter over large areas, or for mountain or high altitude regions and such studies will be addressed during the International Polar Year 2007–2008.

Appendix A

Scavenging coefficient

The below-cloud scavenging coefficient L_{BC} has expression

$$L_{BC}(d_p) = \int_0^{\infty} \frac{\pi}{4} D_p^2 U(D_p) E_{BC}(D_p, d_p) N(D_p) dD_p \tag{A1}$$

where, $U(D_p)$ is the raindrop terminal velocity, $N(D_p)$ is the raindrop size distribution, and $E_{BC}(D_p, d_p)$ is the below-cloud collection efficiency, assumed equal with the collision efficiency (Slinn, 1983). The raindrop terminal velocity is taken as $U(D_p)=c\times D_p^{\gamma}$, with c=3.778 and γ=0.67 (with U in ms^{-1} and D_p in mm) (Atlas and Ulbrich, 1977). The raindrop size distribution is described by an empirical Marshall and Palmer (1948) fit, $N(D_p)=N_0 \exp(-\Lambda D_p)$, where N_0 and Λ depend on rainfall rate R and can exhibit variability from case to case.

For UFP, the below-cloud collection efficiency is

$$E_{BC}(D_p, d_p) = \frac{4}{R_e S_c}(1 + 0.4R_e^{1/2}S_c^{1/3} + 0.16R_e^{1/2}S_c^{1/2}) + 4\frac{d_p}{D_p}[\frac{\mu_a}{\mu_w} + (1 + 2R_e^{1/2})\frac{d_p}{D_p}] + E_e \quad \text{(A2)}$$

where the first six terms represent the Brownian diffusion and interception contributions to the collection efficiency (Slinn, 1977, 1983), and the last term represents the electric contribution. The term E_e is based only on Coulomb interaction between charged aerosols and raindrops treated as in Davenport and Peters (1978). Other notations in the above equation are: $R_e = \frac{D_p U \rho_a}{2\mu_a}$ is the raindrop Reynolds number, $S_c = \frac{\mu_a}{\rho_a D}$ is the aerosol Schmidt number, ρ_a and μ_a are the air density and viscosity, $D = \frac{k_B T C_c}{3\pi\mu_a d_p}$ is aerosol diffusivity in air, k_B is the Boltzmann constant, T is the air absolute temperature, C_c is the Cunningham slip correction factor to account for non-continuum effects associated with small particles, $C_c = 1 + \frac{2\lambda_a}{d_p}[1.257 + 0.4\exp(-\frac{1.1 d_p}{2\lambda_a})]$, and λ_a is the mean free path of air molecules.

The electric term E_e is given by this expression $E_e = \frac{16 K C_c a^2 \alpha^2 d_p}{3\pi\mu_a U}$, with $K = 9\times10^9$ Nm^2 C^{-2} s^{-1}, $a = 0.83\times10^{-6}$, α is an empirical parameter in the relations $Q = a\times\alpha D_p^2$, and $q = a\times\alpha d_p^2$ are the average charges on raindrop and aerosol particle (in C units). α can be varied between 0, which corresponds to neutral particles, to ~7, which corresponds to highly electrified clouds, associated with thunderstorms (Pruppacher and Klett, 1998; Andronache, 2004).

The scavenging coefficient due to in-cloud collection by falling raindrops is

$$L_{IC}^{\text{coll}}(d_p) = \int_0^\infty \frac{\pi}{4} D_p^2 U(D_p) E_{IC} N(D_p) dD_p \quad \text{(A3)}$$

where E_{IC} is the in-cloud collection efficiency between cloud droplets (of diameter 10 μm) and raindrops. E_{IC} is in the range 0.5–0.8 for soluble aerosol scavenged by

liquid drops. For snow, the collection efficiency, E_{IC}~0.2–0.3 (Scott, 1982).

The scavenging coefficient due to in-cloud coagulation between UFP and cloud droplets is

$$L_{IC}^{\text{coag}}(d_p) = \int_0^{\infty} \widetilde{K}(d_c, d_p) n_c(d_c) d d_c \tag{A4}$$

where $\widetilde{K}(d_c, d_p)$ is the Brownian coagulation kernel between UFP and cloud droplets, d_c is the cloud droplet diameter. The coagulation kernel is based on Fuchs (1964). The cloud droplet size distribution is given by $n_c(d_c)=Ad_c^2 \times \exp(-Bd_c)$, with $A=\frac{N_c B^3}{2}$, $B=\frac{3}{\bar{d}_c}$, where $\bar{d}_c$ is the average cloud droplet diameter, and N_c is the total number concentration of cloud droplets (Pruppacher and Klett, 1998).

The calculations are carried out at aerosol particle diameter corrected by a growth factor (GF), determined from observations as a function of particle diameter d_p and ambient relative humidity RH. GF is defined as $GF=\frac{d_p(RH)}{d_p(RH_0)}$, where $d_p(RH)$ is the aerosol diameter at ambient relative humidity RH and $d_p(RH_0)$ is the dry aerosol diameter as measured by the DMPS instrument at $RH \leq 20\%$. A fit of GF that reproduces observations, valid for $RH \leq 99\%$, is given by:

$$GF(RH, d_p) = [1 - RH/100]^{\varepsilon(d_p)} \tag{A5}$$

where $\varepsilon(d_p)=-3.11\times10^5 \times \frac{d_p}{d_{p0}} - 0.0847$, and $d_{p0}=1$ m. For $d_p \geq 280$ nm, $\varepsilon(d_p)=\varepsilon(d_p=280\,\text{nm})$ in this formulation (Laakso et al., 2004).

Appendix B

Notations

d_p	ultrafine particles (UFP) diameter
d_c	cloud droplet diameter
D_p	raindrop diameter
E	collection efficiency
D	aerosol diffusivity in air
f_1	fraction of UFP mixed in-cloud
f_2	in-cloud scavenged fraction of UFP
GF	growth factor of UFP
H	cloud base height
k_B	Boltzmann constant
$K(d_c, d_p)$	Brownian coagulation kernel
L_{eff}	effective scavenging coefficient
L_o	scavenging coefficient from observations
$n(d_p)$	aerosol size distribution
$n_c(d_c)$	cloud droplet size distribution
$N(D_p)$	raindrop size distribution (RSD)
N_0	RSD parameter
R	rainfall rate near ground
R_{IC}	rainfall rate in-cloud
RH	relative humidity
R_e	raindrop Reynolds number
S_c	aerosol Schmidt number
U	raindrop terminal velocity
t_c	air temperature in Celsius degrees
T	air absolute temperature
w_b	entrainment velocity at cloud base
λ_a	mean free path of air molecules
μ_a	air viscosity
ρ_a	air density
ρ_p	aerosol density
Λ	RSD parameter
τ	vertical mixing time scale

Acknowledgements. The authors are grateful to M. Komppula for providing valuable information on cloud droplet activation process measurements and to S. Saku for synoptic weather data analysis.

References

Aalto, P., Hämeri, K., Becker, E., Weber, R., Salm, J., Mäkelä, J. M., Hoell, C., O'Dowd, C. D., Karlsson, H., Hansson, H.-C., Väkevä, M., Koponen, I. K., Buzorius, G., and Kulmala, M.: Physical characterization of aerosol particles during nucleation events, Tellus, 53B, 344–358, 2001.

Alam, A., Shi, J. P., and Harrison, R. M.: Observations of new particle formation in urban air, J. Geophys. Res., 108(D3), 4093, doi:10.1029/2001JD001417, 2003.

Allen, A. G., Grenfell, J. L., Harrison, R. M., James, J., and Evans, M. J.: Nanoparticle formation in marine air masses: Contrasting behavior of the open ocean and coastal environments, Atmos. Res., 51, 1–14, 1999.

Andronache, C.: Estimated variability of below-cloud aerosol removal by rainfall for observed aerosol size distributions, Atmos. Chem. Phys., 3, 131–143, 2003.

Andronache, C.: Diffusion and electric charge contributions to below-cloud wet removal of atmospheric ultra-fine aerosol particles, J. Aerosol Sci., 35, 1467–1482, 2004.

Atlas, D. and Ulbrich, C. W.: Path and area integrated rainfall measurement by microwave attenuation in the 1–3 cm band, J. Appl. Meteorol., 16, 1322–1331, 1977.

Birmilli, W. and Wiedensohler, A.: New particle formation in the continental boundary layer: Meteorological and gas phase parameter influence, Geophys. Res. Lett., 27, 3325–3328, 2000.

Byrne, M. A. and Jennings, S. G.: Scavenging of sub-micrometer aerosol particles by water drops, Atmos. Environ., 27A, 14, 2099–2105, 1993.

Chate, D. M. and Pranesha, T. S.: Field studies of scavenging of aerosols by rain events, J. Aerosol Sci., 35, 695–706, 2004.

Covert, D. S., Kapustin, V. N., Quinn, P. K., and Bates, T. S.: New particle formation in the marine boundary layer, J. Geophys. Res., 97, 20 581–20 589, 1992.

Dana, M. T. and Hales, J. M.: Statistical aspects of the washout of polydisperse aerosols, Atmos. Environ., 10, 45–50, 1976.

Davenport, H. M. and Peters, L. K.: Field studies of atmospheric particulate concentration changes during precipitation, Atmos. Environ., 12, 997–1008, 1978.
Fuchs, N. A.: The mechanics of aerosols, Pergamon Press Ltd, pp. 408, 1964.
Garrett, T. J. and Hobbs, P. V.: Long-range transport of continental aerosols over the Atlantic ocean and their effects on cloud structures, J. Atmos. Sci., 52, 2977–2984, 1995.
Greenfield, S.: Rain scavenging of radioactive particulate matter from the atmosphere, J. Meteorol., 14, 115–125, 1957.
Grover, S. N., Pruppacher, H. R., and Hamielec, A. E.: A numerical determination of the efficiency with which spherical aerosol particles collide with spherical water drops due to inertial impaction and phoretic and electric forces, J. Atmos. Sci., 34, 1655–1663, 1977.
Harrison, R. G. and Carslaw, K. S.: Ion-aerosol-cloud processes in the lower atmosphere, Rev. Geophys., 41(3), 1012, doi:10.1029/2002RG000114, 2003.
Harris, S. and Maricq, M.: Signature size distributions for diesel and gasoline engine exhaust particulate matter, J. Aerosol Sci., 32, 749–764, 2001.
Houze, R. A.: Cloud dynamics, Academic Press, pp. 573, 1993.
Hyvönen, S., Junninen, H., Laakso, L., Dal Maso, M., Grönholm, T., Bonn, B., Keronen, P., Aalto, P., Hiltunen, V., Pohja, T., Launiainen, S., Hari, P., Mannila, H., and Kulmala, M.: A look at aerosol formation using data mining techniques, Atmos. Chem. Phys., 5, 3345–3356, 2005.
Jacobson, M. Z.: Analysis of aerosol interactions with numerical techniques for solving coagulation, nucleation, condensation, dissolution, and reversible chemistry among multiple size distributions, J. Geophys. Res., 107(D19), 4366, doi:10.1029/2001JD002044, 2002.
Jylhä, K.: Empirical scavenging coefficients of radioactive substances released from Chernobyl, Atmos. Environ., 25A, 263–270, 1991.
Kerminen, V.-M. and Wexler, A. S.: The occurrence of sulfuric acid-water nucleation in plumes: Urban environment, Tellus, 48B, 65–82, 1996.
Komppula, M., Lihavainen, H., Kerminen, V., Kulmala, M., and Viisanen, Y.: Measurements of cloud droplet activation of aerosol particles at a clean subarctic background site, J. Geophys. Res., 110, D06204, doi:10.1029/2004JD005200, 2005.
Kulmala, M., Toivonen, A., Mäkelä, J. M., and Laaksonen, A.: Analysis of the growth of nucleation mode particles observed in Boreal forest, Tellus, 50B, 449–462, 1998.
Kulmala, M., Pirjola, L., and Mäkelä, M.: Stable sulfate clusters as sources of new atmospheric particles, Nature, 404, 66–69, 2000a.

Kulmala, M., Rannik, Ü., Pirjola, L., et al.: Characterization of atmospheric trace gas and aerosol concentrations at forest sites in southern and northern Finland using back trajectories, Boreal Env. Res., 5, 315–336, 2000b.

Kulmala, M., Vehkamäki, H., Petäjä, T., Dal Maso, M., Lauri, A. Kerminen, V.-M., Birmili, W., and McMurry, P.: Formation and growth rates of ultrafine atmospheric particles: a review of observations, J. Aerosol Sci., 35, 143–176, 2004.

Laakso, L., Grönholm, T., Rannik, Ü., Kosmale, M., Fiedler, V., Vehkamäki, H., and Kulmala, M.: Ultrafine particle scavenging coefficients calculated from 6 years field measurements, Atmos. Environ., 37, 3605–3613, 2003a.

Laakso, L., Hussein, T., Aarnio, P., Komppula, M., Hiltunen, V., Viisanen, Y., and Kulmala, M.: Diurnal and annual characteristics of particle mass and number concentrations in urban, rural and Arctic environments in Finland, Atmos. Environ., 37, 2629–2641, 2003b.

Laakso, L., Petäjä, T., Lehtinen, K. E. J., Kulmala, M., Patatero, J., Hörrak, U., Tammet, H., and Joutsensaari, J.: Ion production rate in a boreal forest based on ion, particle and radiation measurements, Atmos. Chem. Phys., 4, 1933–1943, 2004.

Mäkelä, J. M., Dal Maso, M., Pirjola, L., Keronen, P., Laakso, L., Kulmala, M., and Laaksonen, A.: Characteristics of the atmospheric particle formation events observed at a boreal forest site in southern Finland, Boreal Env. Res. 5, 299–313, 2000.

Maria, S. S. and Russell, L. M.: Organic and Inorganic Aerosol Below-Cloud Scavenging by Suburban New Jersey Precipitation, Environ. Sci. Technol., 39(13) 4793–4800, 2005.

Marshall, J. S. and Palmer, W. M.: The distribution of raindrop with size, J. Meteorol., 5, 165–166, 1948.

Martin, G. M., Johnson, D. W., and Spice, A.: The measurement and parameterization of effective radius of droplets in warm stratocumulus clouds, J. Atmos. Sci., 51, 1823–1842, 1994.

Martinsson, B. G., Frank, G., Cederfelt, S. I., et al.: Droplet nucleation and growth in orographic clouds in relation to aerosol population, Atmos. Res., 50, 289–315, 1999.

McGann, B. T. and Jennings, S. G.: The efficiency with which drizzle and precipitation sized drops collide with aerosol particles, Atmos. Environ., 25A, 3/4, 791–799, 1991.

O'Dowd, C., McFiggins, G., Creasey, D. J., Pirjola, L., Hoell, C., Smith, M. H., Allan, B. J., Plane, J. M. C., Heard, D. E., Lee, J. D., Pilling, M. J., and Kulmala, M.: On the photochemical production of new particles in the coastal boundary layer, Geophys. Res. Lett., 26, 1707–1710, 1999.

Pimenoff, N., Grönholm, T., Rinne, J., Helenelund, C., Kulmala, M., and Vesala, T.: Carbon dioxide flux and aerosol particle concentration measurements using a tethered balloon, Report Series in aerosol Science, 73, Research Unit on Physics, Chemistry and Biology of Atmospheric Composition and Climate Change: III Progress Report and Proceedings of Seminar in Pallas, 29 March–1 April 2005, 223–227, 2005.

Pruppacher, H. R. and Klett, J. D.: Microphysics of clouds and precipitation, Kluwer Academic Publishers, Dordrecht, Boston, London, pp. 954, 1998.

Raes, F., Van Dingenen, R., Cuevas, E., Van Velthoven, P. F. J., and Prospero, J. M.: Observations of aerosols in the free troposphere and marine boundary layer of the subtropical Northeast Atlantic: Discussion of processes determining their size distribution, J. Geophys. Res., 102, 21 315–21 328, 1997.

Rasch, P. J., Feichter, J., Law, K., et al.: A comparison of scavenging and deposition processes in global models: results from the WCRP Cambridge Workshop of 1995, Tellus, 52B, 1025–1056, 2000.

Rutledge, S. A. and Hobbs, P. V.: The mesoscale and microscale structure and organization of clouds and precipitation in midlatitude cyclones. VIII: A model for the feeder-seeder process in warm frontal rainbands, J. Atmos. Sci., 40, 1185–1206, 1983.

Schumann, T.: Aerosol and hydrometeor concentrations and their chemical composition during winter precipitation along mountain slope – III. Size-differentiated in-cloud scavenging efficiencies, Atmos. Environ., 25A, 3/4, 809–824, 1991.

Scott, B. C.: Theoretical estimates of the scavenging coefficient for soluble aerosol particles as a function of precipitation type, rate, and altitude, Atmos. Environ., 16, 7, 1753–1762, 1982.

Seinfeld, J. H. and Pandis, S. N.: Atmospheric Chemistry and Physics, Wiley, New York, 1326 pp., 1998.

Slinn, W. G. N. and Hales, J. M.: A reevaluation of the role of thermophoresis as a mechanism of in- and below-cloud scavenging, J. Atmos. Sci., 28, 1465–1471, 1971.

Slinn, W. G. N.: Some approximations for the wet and dry removal of particles and gases from the atmosphere, Water, Air, and Soil Pollut., 7, 513–543, 1977.

Slinn, W. G. N.: Precipitation scavenging, in: Atmospheric Sciences and Power Production – 1979, chap. 11, Division of Biomedical Environmental Research, U.S. Department of Energy, Washington, D.C., 1983.

Snider, J. R. and Brenguier, J. L.: Cloud condensation nuclei and cloud droplet measurements during ACE-2, Tellus B, 52, 828–842, 2000.

Sparmacher, H., Fulber, K., and Bonka, H.: Below-cloud scavenging of aerosol particles: Particle-bound radionuclide – Experimental, Atmos. Environ., 27A, 4, 605–618, 1993.
Svenningsson, B., Hansson, H.-C., Martinsson, B., et al.: Cloud droplet nucleation scavenging in relation to the size and hygroscopic behavior of aerosol particles, Atmos. Environ., 31, 16, 2463–2475, 1997.
Swietlicki, E., Zhou, J., Berg, O. H., et al.: A closure study of sub-micrometer aerosol particle hygroscopic behavior, Atmos. Res., 50, 205–240, 1999.
Ten Brink, H. M., Schwartz, S. E., and Daum, P. H.: Efficient scavenging of aerosol sulfate by liquid-water clouds, Atmos. Environ., 21, 9, 2035–2052, 1987.
Tinsley, B. A., Rohrbaugh, R. P., Hei, M., and Beard, K. V.: Effects of image charges on scavenging of aerosol particles by cloud droplets and on droplet charging and possible ice nucleation processes, J. Atmos. Sci., 57, 2118–2134, 2000.
Tripathi, S. N. and Harrison, R. G.: Scavenging of Radioactive Aerosol, Atmos. Environ., 35, 5817–5821, 2001.
Tost, H., Jöckel, P., Kerkweg, A., Sander, R., and Lelieveld, J.: Technical note: A new comprehensive SCAVenging submodel for global atmospheric chemistry modeling, Atmos. Chem. Phys., 6, 565–574, 2006.
Twohy, C. H., Durkee, P. A., Huebert, B. J., and Charlson, R. J.: Effects of aerosol particles on the microphysics of coastal stratiform clouds, J. Climate, 8, 773–783, 1995.
Vesala, T., Haataja, J., Aalto, P., Altimir, N., Buzorius, G., et al.: Long-term field measurements of atmosphere – surface interactions in boreal forest ecology, micrometeorology, aerosol physics and atmospheric chemistry. Trends in Heat, Mass and Momentum Transfer, 4, 17–35, 1998.
Wang, P. K. and Pruppacher, H. R.: An experimental determination of the efficiency with which aerosol particles are collected by water drops in subsaturated air, J. Atmos. Sci., 34, 1664–1669, 1977.
Wang, P. K., Grover, S. N., and Pruppacher, H. R.: On the effect of electric charges on the scavenging of aerosol particles by clouds and small raindrops, J. Atmos. Sci., 35, 1735–1743, 1978.
Weber, J. R., McMurry, P. H., Mauldin, L., et al.: A study of new particle formation and growth involving biogenic and trace gas species measured during ACE1, J. Geophys. Res., 103, 16 385–16 396, 1998.
Wiedensohler, A., Covert, D. S., Swietlicki, E., Aalto, P., Heintzenberg, J., and Leck, C.: Occur-

rence of an ultrafine particle mode less than 20 nm in diameter in the marine boundary layer during Arctic summer and autumn, Tellus, 48B, 213–222, 1996.
Yu, F. and Turco, R.: From molecular clusters to nanoparticles: Role of ambient ionization in tropospheric aerosol formation, J. Geophys. Res., 106, 4797–4814, 2001.
Zhang, L., Michelangeli, D. V., and Taylor, P. A.: Numerical studies of aerosol scavenging by low-level, warm stratiform clouds and precipitation, Atmos. Environ., 38, 4653–4665, 2004.

Table 1. Model parameters and their values used in the reference run and in sensitivity calculations.

Parameter	Reference run	Range	Notes
t_c	10 (degC)	0–20 (degC)	(a)
RH	90 %	60–99%	(b)
N_0	$8\times10^6\,\mathrm{m}^{-4}$	$[8–80]\times10^6\,\mathrm{m}^{-4}$	(c)
N_c	$500\,\mathrm{cm}^{-3}$	$500–1500\,\mathrm{cm}^{-3}$	(d)
f_1	0.1	0.1–0.3	(e)
E_{IC}	0.5	0.3–0.9	(f)

(a) Air temperature at 8.4 m above ground was in the range [0–20] degC, with values mostly being ∼10 degC (Laakso et al., 2003a); (b) Most samples have relative humidity $RH\geq60\%$ with predominant values $RH\geq90\%$; (c) N_0, the intercept parameter in the Marshall and Palmer raindrop size distribution can vary significantly; (d) Number concentration of cloud droplets was varied between clean continental to polluted conditions; (e) Fraction of UFP mixed into cloud elements was varied between 0.1 and 0.3; (f) In-cloud collection efficiency was varied between 0.3 (for less soluble aerosols) and 0.9 (highly soluble aerosols);

Table 2. Range of reported aerosol scavenging coefficient determined from measurements of the size distribution during rain events.

L_o (s^{-1})	R ($mm\,h^{-1}$)	Location	Reference
2×10^{-5}–1×10^{-4}	1–3	Lexington, Kentucky, USA	Davenport and Peters (1978)[a]
7×10^{-6}–4×10^{-5}	0.5–10	Hyytiälä, Finland	Laakso et al. (2003a)[b]
1×10^{-5}–8×10^{-4}	1–46	Pune, India	Chate and Pranesha (2004)[c]
4×10^{-5}–1×10^{-4}	1–20	Princeton, New Jersey, USA	Maria and Russell (2005)[d]

[a] Experiments were conducted during three rain events on 1 September, 25 October and 30 October 1976. The rain events were widespread precipitation. Aerosol measurements were limited to two subranges of the size distribution: one with d_p in the range [7–22] nm, and the other with $d_p \geq 400$ nm.

[b] Measurements were taken during May–October months, 1996–2001. Aerosol size distribution measured for d_p in the range [3–510] nm. Rain events were characterized by predominant low intensities (see text for details).

[c] Measurements were taken during a total of 17 rain events: two days in the pre-monsoon season in April 1997, and ten days post-monsoon during October and November 1997. Eight aerosol particle sizes with d_p in the range [13–750] nm were used in the experiment. Precipitations were dominated by strong convective activity and thunderstorms.

[d] Observations were conducted during 10-day period in August 2003. Particle sizes measured ranged between 10 nm and 20 000 nm. Precipitation rate varied between 1 and 20 $mm\,h^{-1}$.

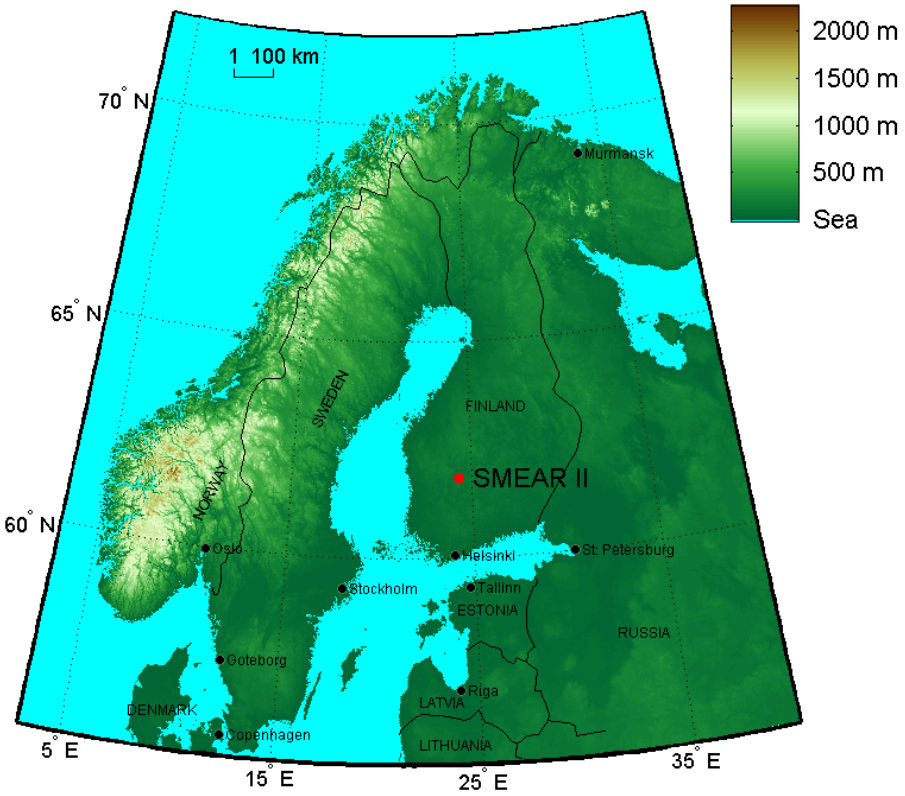

Fig. 1. Regional map with position of the observation site, SMEAR II in Southern Finland.

ACPD
6, 3801–3844, 2006

EGU

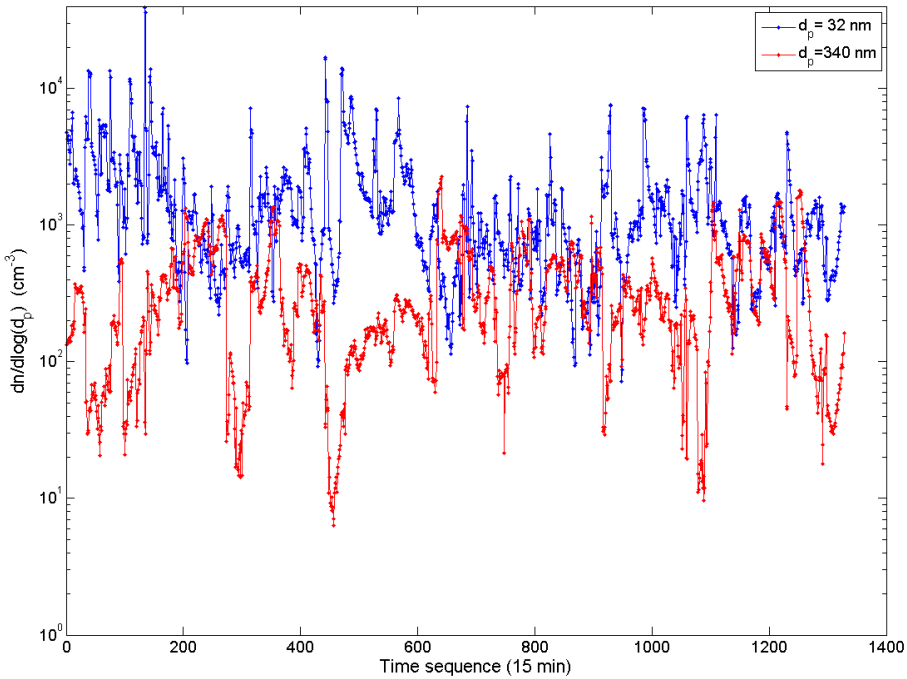

Fig. 2. Time sequence of measured dn/d[log(d_p)] for two particle diameters. Samples shown are from rainy events during months May–October 2000. Dry time intervals are excluded from this plot, and the continuous lines are shown for figure clarity.

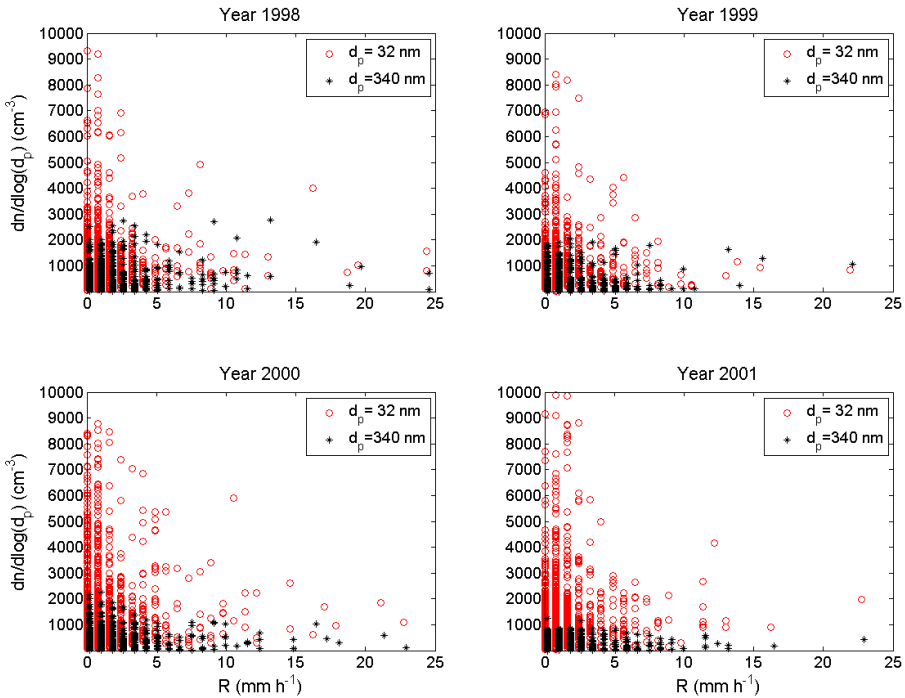

Fig. 3. Scatterplot of the measured dn/d[log(d_p)] (for two values of UFP diameter) versus rainfall rate R during years 1998–2001.

ACPD
6, 3801–3844, 2006

EGU

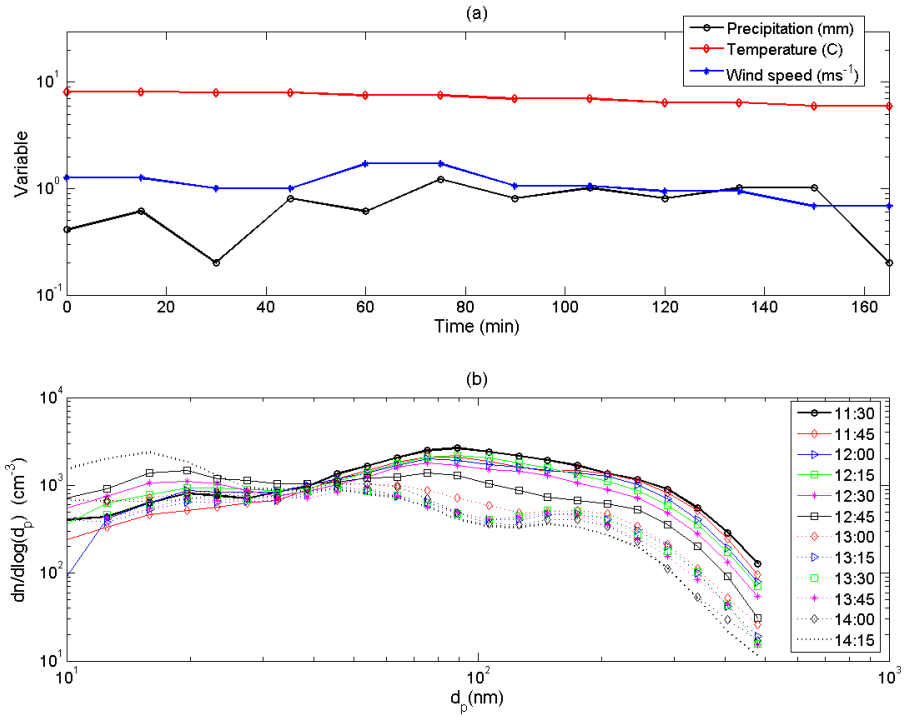

Fig. 4. **(a)** Observed meteorological parameters at 8.4 m above ground, and **(b)** aerosol size distribution versus local time during a precipitation event on 9 October 1999.

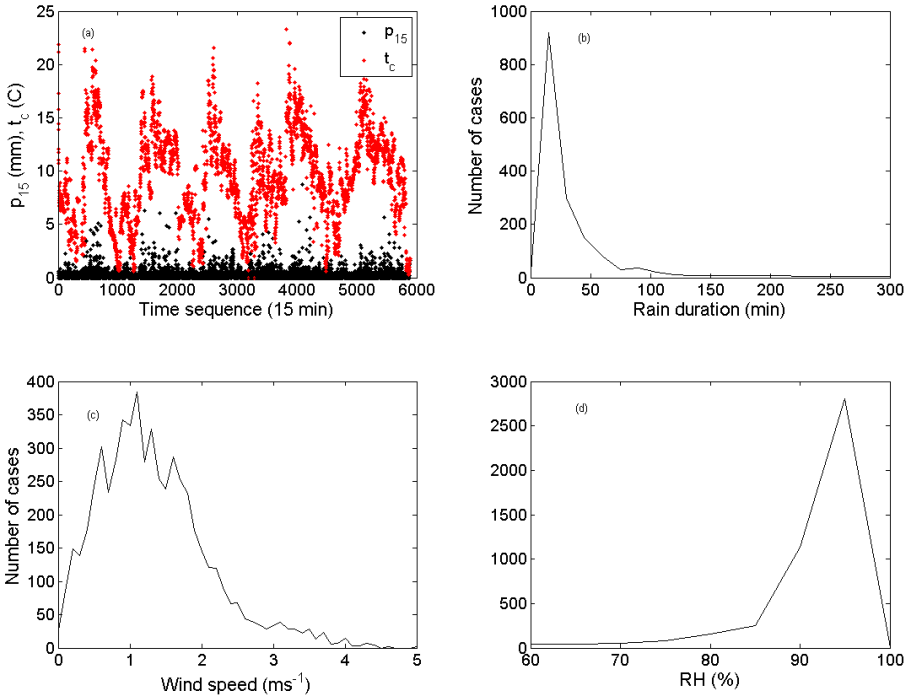

Fig. 5. Observed meteorological parameters at 8.4 m above ground at Hyytiälä: **(a)** Time sequence of air temperature and precipitation recorded during precipitation events, for May–October interval, during years 1996–2001. Dry periods are excluded from this plot; **(b)** Frequency of rain duration; **(c)** Frequency of horizontal wind intensity; **(d)** Frequency of relative humidity, *RH*.

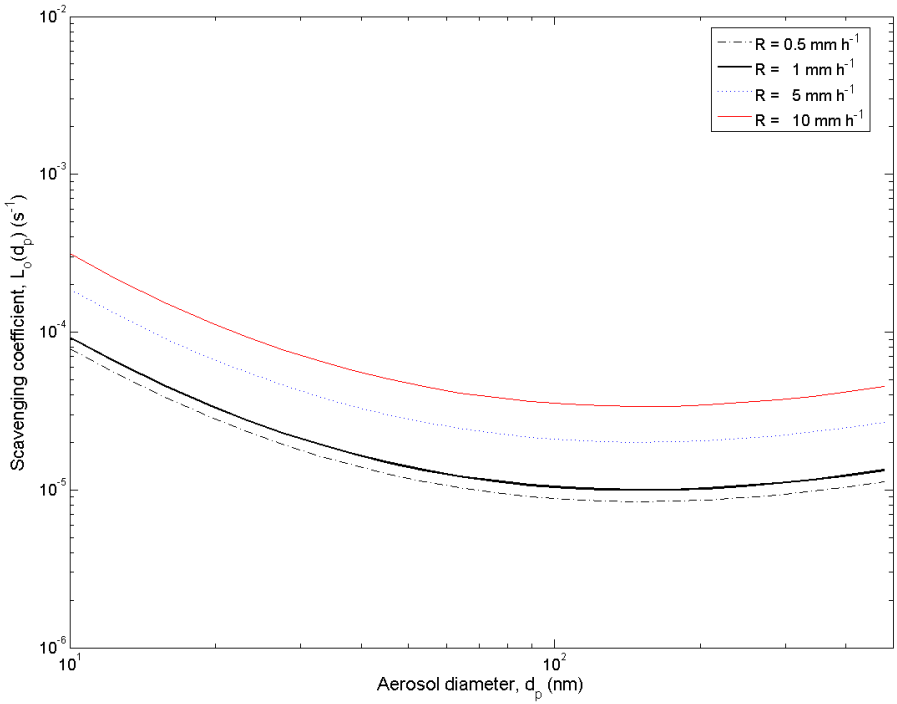

Fig. 6. Fit of the scavenging coefficient from observations, L_o, versus aerosol particle, for several representative rainfall intensities, R.

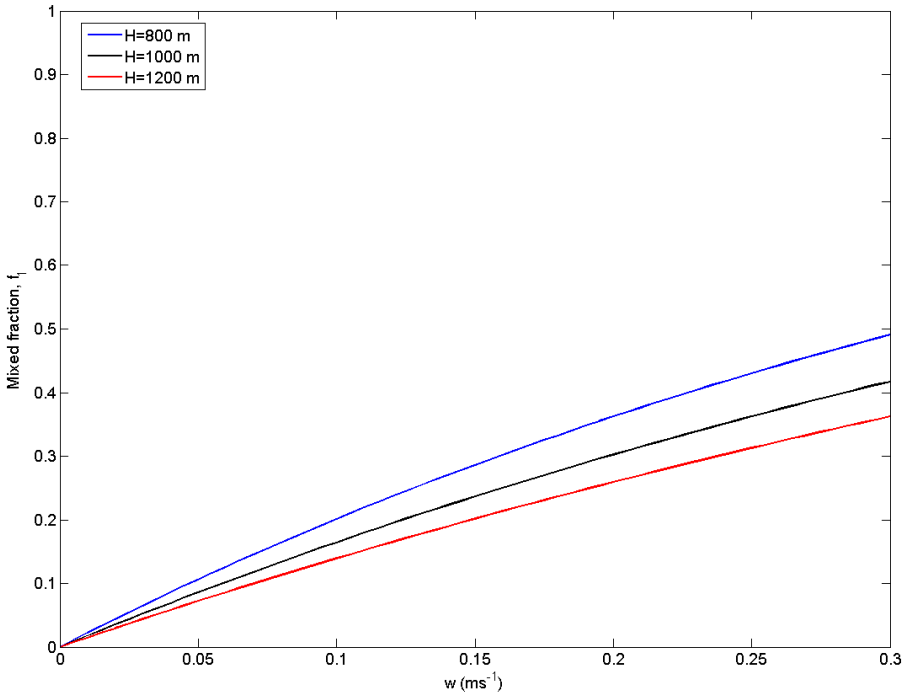

Fig. 7. Mixed fraction f_1 of ultrafine particles into cloud versus the average vertical velocity in the boundary layer. H is the average cloud base height.

ACPD
6, 3801–3844, 2006

EGU

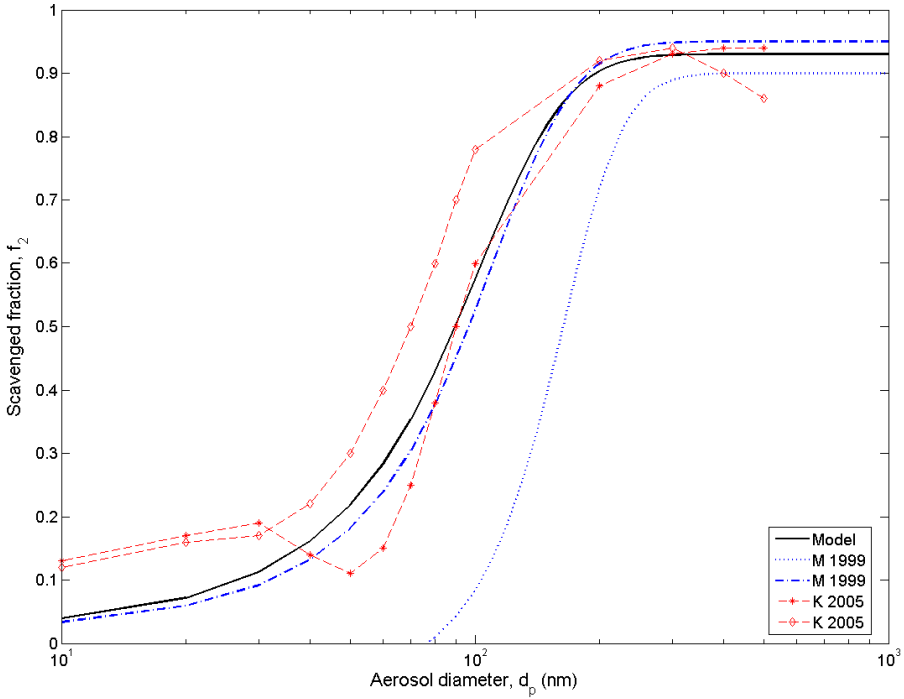

Fig. 8. Scavenged fraction f_2 of UFP mixed into cloud. The black curve is the function used in the model runs shown in results, while the dotted curves represent the boundaries which contain the scavenged fraction determined from observations by Martinsson et al. (1999) (M 1999) and Komppula et al. (2005) (K 2005).

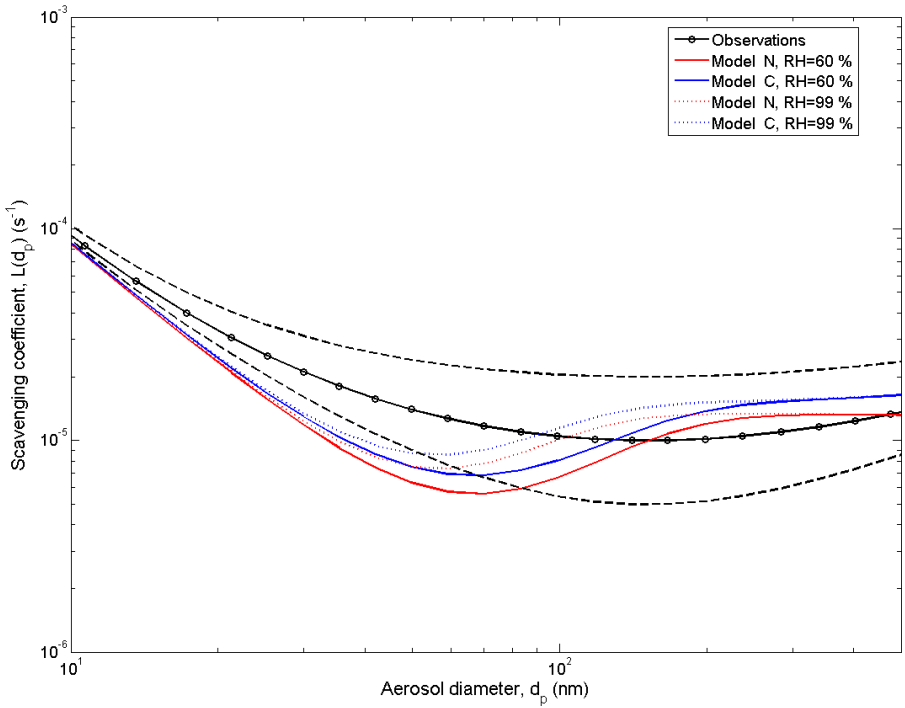

Fig. 9. Scavenging coefficient versus UFP diameter. Shown are L_o from observations, and L_{eff} model calculated for neutral (N) and charged (C) particles, for two relative humidity values, RH=60% and RH=99%. The two black dashed lines represent the uncertainties of the scavenging coefficient from observations.

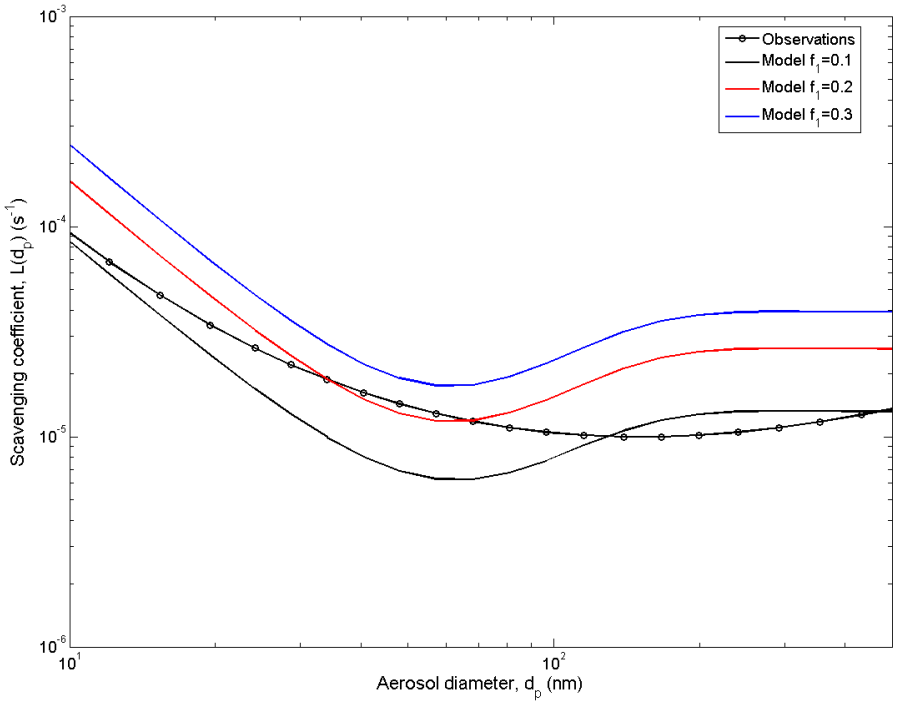

Fig. 10. Sensitivity of model results to the fraction of UFP mixed into cloud, f_1.

ACPD
6, 3801–3844, 2006

EGU

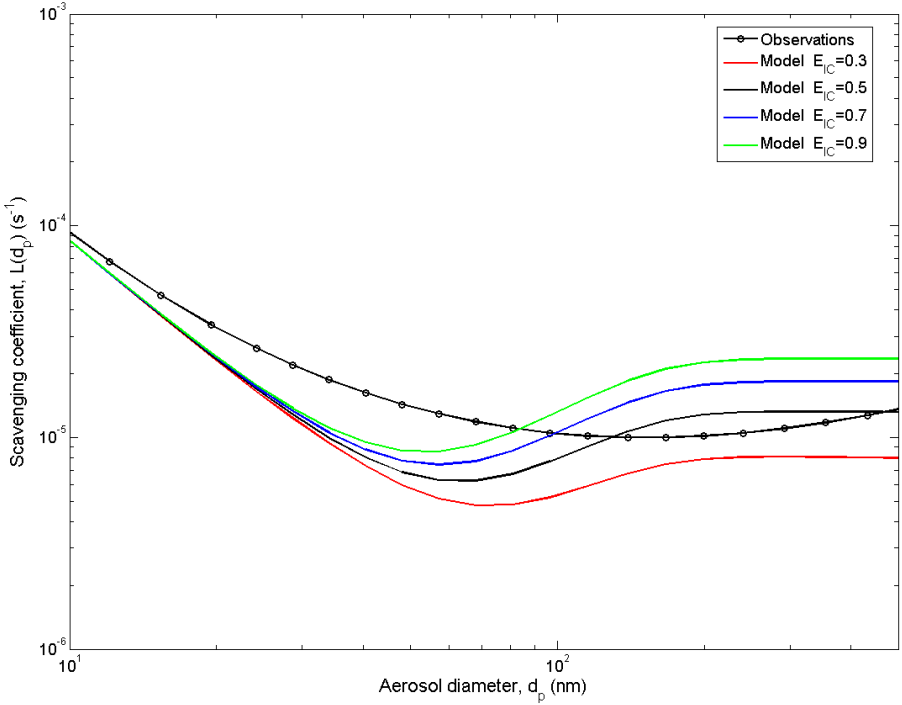

Fig. 11. Sensitivity of model results to in-cloud efficiency of collection (E_{IC}) between cloud droplets and falling raindrops.

ACPD
6, 3801–3844, 2006

EGU

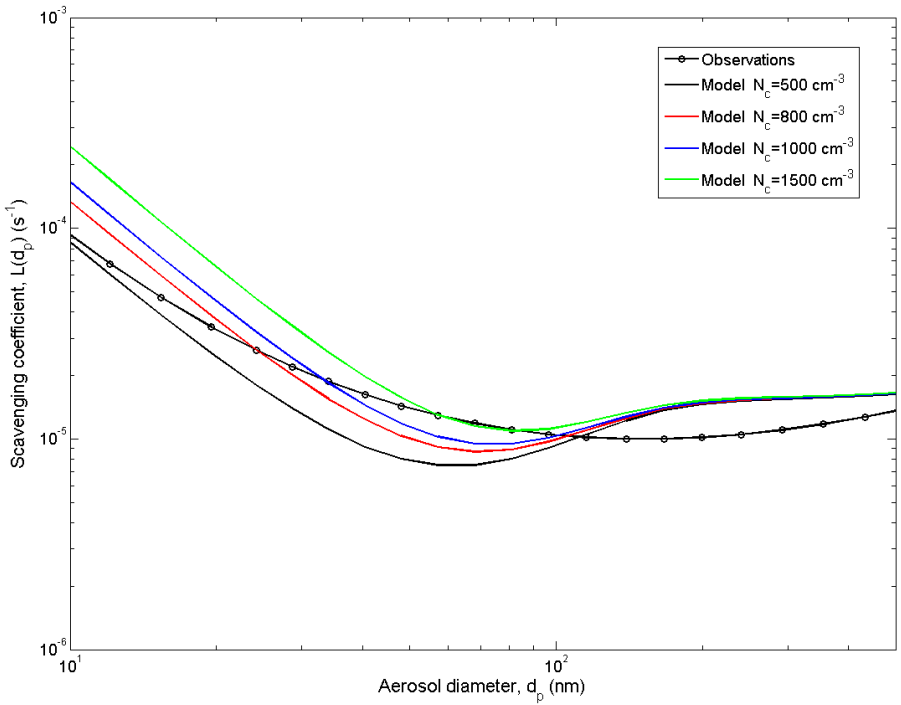

Fig. 12. Sensitivity of model results to cloud droplet number concentration, N_c.

ACPD
6, 3801–3844, 2006

EGU

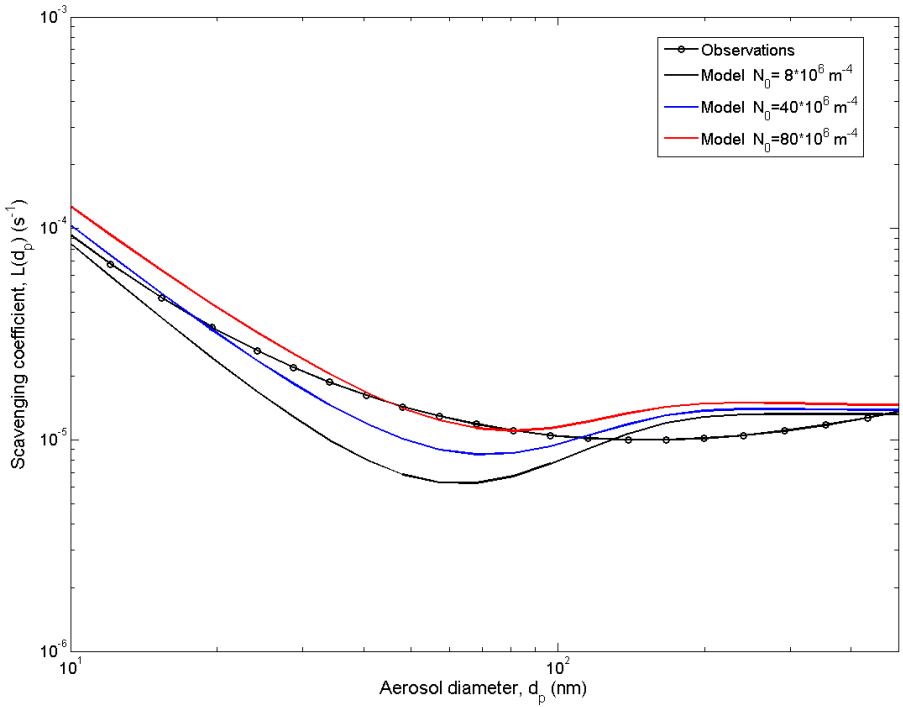

Fig. 13. Sensitivity of model results to Marshall and Palmer raindrop size distribution intercept parameter, N_0.